History of Medicine, 2023, 9(2): 189–197
DOI: 10.17720/2409-5834.v9.2.2023.029

Synthesized, optical properties and biological activity of copper oxide nanoparticles prepared by various parameters of laser ablation technique in DDW

Khalaf Ajaj[1], Abdullah. M. Ali[2]

[1]*Department of Physics, College of Education for Pure Sciences, University of Tikrit , Iraq . Ministry of Education, 41001 Mosul, Iraq*
Email: khalafajaj1@gmail.com
Email: khalaf.aj.hussein@st.tu.edu.iq
[2]*Professor in Department of Physics , College of Education for Pure Sciences , University of Tikrit , Iraq*
Email: Abdullah.ma1763@tu.edu.iq

Received: 11 May 2023 **Accepted:** 10 June 2023

Citation: Ajaj K, Ali AM (2023) Synthesized, optical properties and biological activity of copper oxide nanoparticles prepared by various parameters of laser ablation technique in DDW. History of Medicine 9(2): 189–197. https://doi.org/10.17720/2409-5834.v9.2.2023.029

Abstract

In this paper, copper oxide nanoparticles were prepared through Q-switched Nd:YAG laser ablation. The ablation process was carried out on a copper pellet that was submerged in double-distilled water. The ablation was performed at two different energy levels, specifically 200 mJ and 400 mJ, and with varying numbers of pulses ranging from 100 to 500 by step 100. The morphological and optical characteristics of nanoparticles were ascertained through the utilization of a UV-Vis spectrophotometer, transmission electron microscopy (TEM) and atomic force microscopy (AFM). As the laser pulses were increased, surface plasmon resonance peaks were observed in the absorption spectra at 217 nm. Additionally, there was a slight decrease in the optical band gap. The results of the UV-vis and TEM analyses indicated the presence of CuO nanoparticles that were almost spherical in shape. The average diameter of these nanoparticles was found to be about 46 nm and 52 nm when the energies used were 200 mJ and 400 mJ, respectively. It is noteworthy that the particle size of CuONPs was increased by increasing the laser energy of ablation .Moreover, the findings of our investigation indicate that the inhibitory effect against both Bacillus cereus and Pseudomonas aeruginosa, respectively, was enhanced by CuONPs at 200 mJ in comparison with 400 mJ with the same number of pulses.

Keyword:

Laser ablation, Copper oxide NPs, Optical characteristics, Morphology of CuO, Antibacterial activity.

In recent years have seen a lot of interest in transition metal oxide nanostructures because of their unique mechanical, electrical, optical, and magnetic properties (Zhang et al.,2014). Due to the applications in chemistry, physics, biology, material science, medicine, and catalysis, nanoscale materials are an important subject in basic and applied sciences (Mafuné et al.,2001).Copper nanoparticles(CuNPs) have recently attracted attention due to their low cost and antibacterial properties, making them one of the most important alternatives to silver nanoparticles(Bhardwaj et al.,2019). Metal NPs are created using a variety of techniques, including laser ablation, chemical reduction, photo-reduction, microorganism arc discharge, and bio surfactant. The laser ablation in liquid technique (PLAL) is a clean and green approach for the synthesis compared to other conventional technique for preparing metal colloids, the absence of chemical reagents in solutions distinguishes this technique and has gained popularity and is widely used to synthesize novel

materials such as metal and metal oxide nanostructures (Arakelyan et al.,2016; Menazea et al.,2018). In order to laser ablate a solid target submerged in liquid, a pulsed laser beam must be focused on the target's surface and heats up to high temperature. The surface of the solid target is abraded instantly to produce plasma, which is known as laser-induced plasma. As result molten droplets (NPs) can be ejected from a heated target. Through the manipulation of laser parameters such as wavelength, laser pulse energy and pulse duration, as well as liquid medium properties, this method can also control the size and shape of the nanoparticles (Ganeev et al.,2004; Giorgetti et al.,2015;Patra et al.,2016; Al-Douri et al.,2019). Using pulsed laser ablation of copper target in liquid media, colloidal oxide copper (CuONPs) are synthesized. CuO NPs demonstrated anticancer, antioxidant, antibacterial activity and drug delivery properties, making them a promising tool for biomedical applications (Kareem,2021). Additionally, CuO Nanostructured are exceptionally versatile are used in other applications , such as biosensors, gas sensors, electrode materials of lithiumion batteries, photo-detectors and supercapacitors (Zoolfakar et al.,2014;Azadi et al.,2019). Optical fields are capable of inducing the collective oscillation of electrons on metal surfaces is known as surface plasmon resonance (SPR).The amplitude of SPR is related to the size of the particle (Nie and Emory,1997). On the other hand, The study of spore-forming bacteria as etiological agents of foodborne illness has increased in importance as a result of the lengthening of the shelf lives of refrigerated processed foods and the steady increase in the population of older and sicker individuals. An emerging foodborne pathogen is Bacillus cereus, a gram-positive bacterium that produces toxins and forms endospores because its spores can withstand both heat and acid(Dufrenne et al.,1994; Carlin et al.2006). Between 1998 to 2000, B. cereus was responsible for up to 60% of outbreaks of foodborne B. cereus infection caused by mass catering facilities. Additionally, pseudomonas aeruginosa is a prominent causative agent among infections attributed to Gram-negative rods. The effective management of infections caused by Gram-negative pathogens poses a significant challenge for medical practitioners, owing to the escalating levels of antimicrobial resistance in healthcare environments (Pena et al.,2009; El Zowalaty et al.,2015). Due to the development of antibiotic resistance, the use of nanoparticles as new agents for microbial growth inhibition has increased (Monteiro et al.,2009; Allaker,2010). The copper oxide nanoparticles exhibited inhibitory effects toward both groups of bacteria, depending on the particle size, such as (B. subtilis , S. aureus) which are gram-positive, and (E. coli , P. aeruginosa) which are gram-negative (Azam et al.,2012; Halbus et al.,2019) .

The present study involves the synthesis of copper oxide nanoparticles using the PLAL technique, with the control of ablated energies and pulse counts. The optical and Morphology properties of the prepared samples were investigated using UV-Visible spectrophotometer, transmission electron microscopy and atomic force microscopy. Furthermore. CuONPs were used to investigate the antibacterial efficacy against Bacillus cereus and pseudomonas aeruginosa.

2. Experimental Methods

2.1. Materials and methods:

CuO nanoparticles colloidal solutions were prepared in liquid using a pulsed laser ablation technique (PLAL). At a distance of 10 cm from the laser source, a high purity cooper plate (99.99%) of a disc-shaped target with a diameter of 20 mm and a thickness of 2 mm was placed in a beaker containing 5 ml of double distilled water (DDW). **Fig.1** depicts the PLAL experimental setup. Q-switched Nd: A YAG laser with a repetition rate of 6 Hz, a wavelength of 1064 nm, and a pulse width of 10 ns was used. At room temperature and ambient pressure, the laser source operated at two different energies (200 and 400 mJ), and the number of pulses was varied from 100 to 500 by a step of 100 pulses for each energy. Before ablation, the target was washed several times with deionized water, acetone, and ethanol to remove the oxide layer formed by air exposure and placed in an ultrasonic bath to replace mechanical impurities. During the ablation procedure, the beaker was slowly rotated to avoid craters being formed on the target surface by the focused beam and to disperse the produced NPs through liquid movement. PLAL produces the ejection of NPs in the form of colloidal solutions.

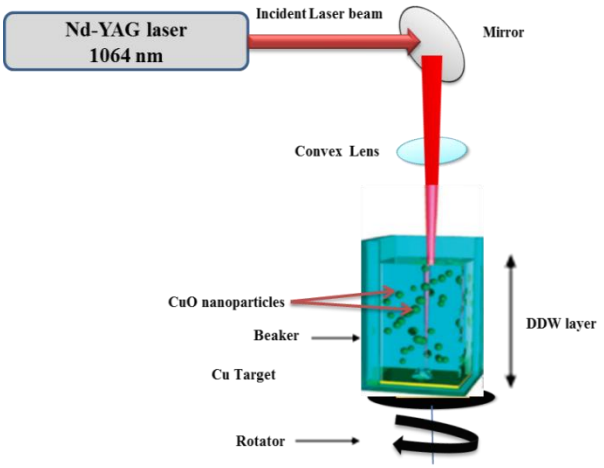

Fig.1. Schematic diagram of PLAL system.

Agar well diffusion method and Antibacterial activity of CuONPs

One liter of distilled water was used to dissolve 37 grams of Mueller Hinton agar (MHA) to create a medium. The pH was adjusted to 7.2, and the medium was sterilized using a sterilization device known as a syringe (autoclave). Next, it is poured into disposable Petri dishes, which are placed on a level surface to a depth of approximately 4 mm, and stored in the refrigerator at 277 k until it is used. Two bacterial strains, Bacillus cereus (Gram-positive) and pseudomonas aeruginosa (Gram-negative), were used to evaluate the antibacterial activity for 200 and 400 mJ of CuONPs with 500 pulses of samples. Using sterile cotton swabs, the bacteria were planted and thoroughly wiped on the plates' media in this method. Then, 150 µl of a solution containing copper oxide NPs was added to each type of bacteria's prepared spot. The plates containing the test organism and CuONPs were then incubated at 310 k for 24 hours. After incubation, the effect of CuONPs on the growth of bacteria was examined by observing the inhibition zone and the surface's transformation into a transparent layer, which indicated the inhibition of bacterial growth.

3.Results and discussions

3.1. The Optical absorption analysis

Spectroscopic absorption of synthesized colloidal solution of copper oxide NPs in DDW is investigated using a UV-Vis spectrophotometer. Optical properties can be studied by observing the interaction between light and metal. The absorption spectra of colloidal NPs exhibit absorbance variation as a function of wavelength. The increase in absorption as the number of laser pulses increases indicates an increase in CuONPs concentration, as shown in **Fig.2** . CuO nanoparticles are present when the peak of the surface plasmon resonance rises. Furthermore. As the number of laser pulses increased , the peak became narrower and the size of CuONPs grew. On the basis of the presence of a plasmon band, spherical CuONPs were fabricated. Because of plasmon absorption, the color of colloidal CuO nanoparticles changed to a light green as shown in **Fig.3** .The SPR band is affected by particle size, which red shifts it to in the visible spectrum is toward the longer wavelength. In addition, the NPs exhibit a low absorption value (high transmission T) on the higher wavelength side, which includes the visible spectrum and wavelengths up to 500 nm. The phenomenon of low absorption can be explained by the fact that the energy of the incident photon decreases with increasing wavelength and cannot interact with the atoms of colloidal media. Therefore, the photons will be transmitted rather than absorbed. CuO nanoparticles may be formed by two common processes, the thermal evaporation of atomic (and ionic) species from the liquid-solid interface and the thermally induced discharge of nanometer-sized molten droplets from the target. At the interface of liquid and target, the adiabatic expansion of the created plasma confines the surrounding double distilled water. The presence of PLAL in DDW solution results in an oxygen-rich cavitation bubble environment. Plasma's high temperature and pressure create the chemical conditions for the formation of CuO. Therefore, species within the plasma plume can interact to produce CuO nanoparticles. Eventually, the plasma is extinguished, and the CuO structures solidify(Zeng et al.,2005;2009) . In addition, DDW can react with molten particles, and molten Cu oxidation contributes to the formation of CuO. Consequently, both of these phenomena may be responsible for the formation of CuO structures(Niu et al.,2010;Gondal,et al.,2013).

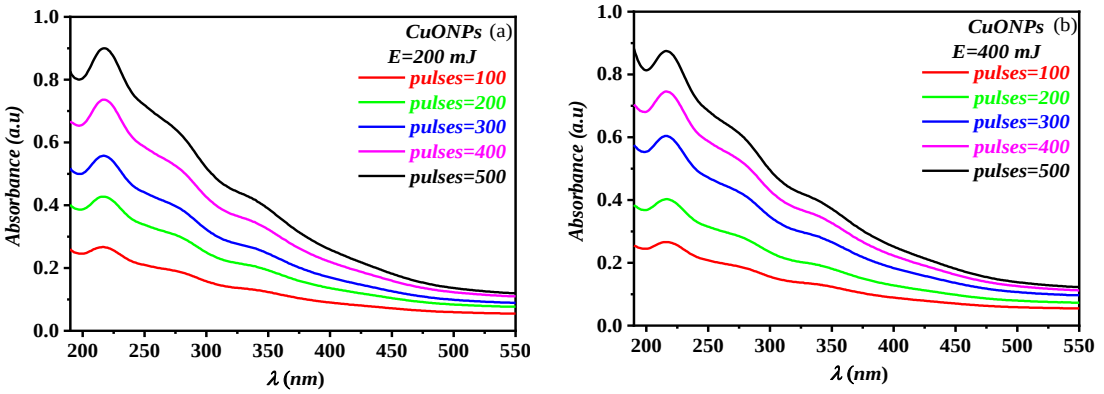

Fig.2. Absorption spectra of CuONPs in DDW at various number of pulses (100,200,300,400, and 500) and different pulse energies (200 and 400) mJ.

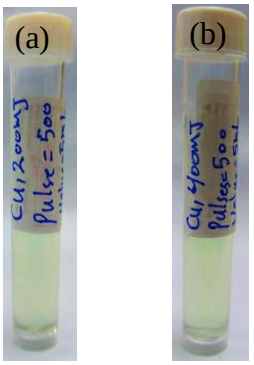

Fig. 3. Photograph of the CuONPs colloidal solutions obtained by laser ablation using different energies (a) 200 and (b) 400 mJ at the same number of pulses 500

By fitting Tauc's relation (Tauc et al,1966) , the optical band gap was calculated using linear extrapolation of the equation's (α.hv) versus (hv) curve. based on the absorption coefficient calculated as a function of photon energy of incident is used to calculate the direct optical band gap $E_g^{opt.}$ of CuO nanoparticles prepared by 500 pulses and different pulse energies: (200 and 400) mJ of Nd:YAG laser in DDW.

$$(\alpha.\mathrm{hv})^{1/2} = \mathrm{B}\left(\mathrm{hv} - \mathrm{E_g}^{\mathrm{opt.}}\right) \qquad (1)$$

where **hυ** is the photon energy, **B** is a constant.

The incident photon energy and the material's properties affect the absorption coefficient (α) and has also been calculated using the relationship below, which is dependent on the absorbance A (Triloki et al,2013)

$$\alpha = \frac{2.303\ \mathrm{A}}{\mathrm{t}} = \frac{2.303}{\mathrm{t}} \log \frac{\mathrm{I_o}}{\mathrm{I}} \qquad (2)$$

Where I_o and I are the incidence and transmission intensities of light, respectively and t is the thickness. The optical band gap of CuONP has been estimated using UV-Visible spectroscopy, as shown in **Figs. 4 and 5 ,** It has been that $E_g^{opt.}$ slight decrease as the number of pulses increases. This result corresponds to the behavior observed in the absorption spectra. This increase is due to the quantum confinement effect. The CuONPs removed from the target at higher ablation energy 400 mJ is larger more than that at 200 mJ with a fixed number of pulses.

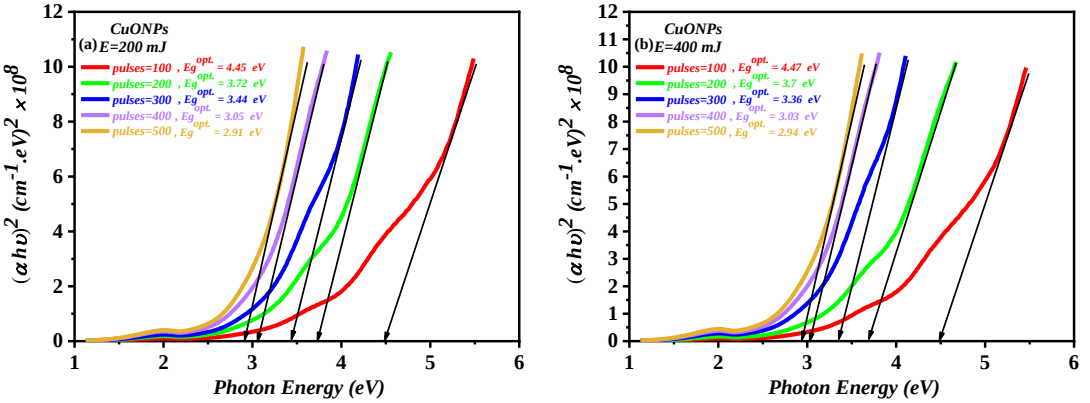

Figs. 4. (αhν)2 versus hν plot for CuONPs prepared at different number of pulses and different pulse energies

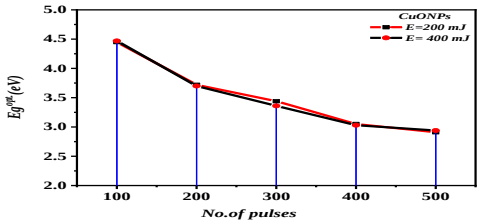

Figs. 5. Optical band gap values as a function the number of pulses for prepared CuONPs at different energies.

The absorption coefficient (α) increases as the number of laser pulses due to an increase in the concentration of CuONPs and increased electronic excitation in CuONPs , as shown in **Fig. 6.**

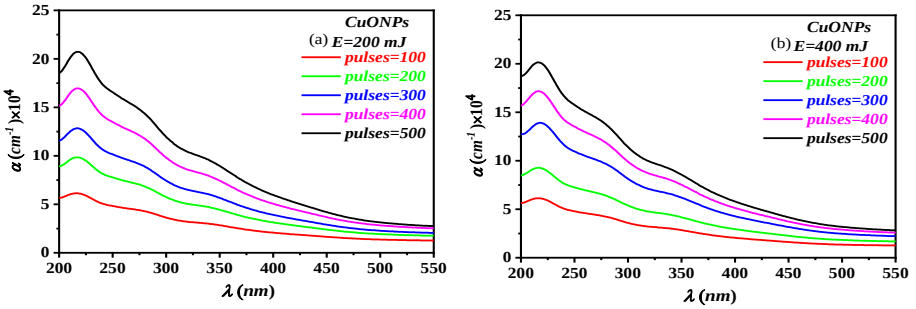

Fig.6. Absorption coefficient as a function of wavelength of CuONPs at different energies for different pulse ratings ((a) 200 mJ and (b)400mJ).

3.2. Morphology and particles size analysis for Synthesized of CuONPs

3.2.1.Transmission electron microscopy(TEM) analysis

The confirmation of the average particle size, size distribution, and morphology of individual CuONPs (200 and 400)mJ with 500 pulses prepared by PLAL technique has been achieved through the utilization of transmission electron microscopy analysis. TEM image analysis by using (image J) program. It is clear from the TEM image in **Fig. 7.**, the aforementioned NPs exhibit a nearly spherical morphology. The diameters of the CuONPs verified from the TEM image in the range of 44 to 51 nm. On the other hand, The agglomeration of nanoparticles can be attributed to the lack of anti-agglomeration agents in the colloidal aqueous solution, as metal nanoparticles have a tendency to agglomerate.

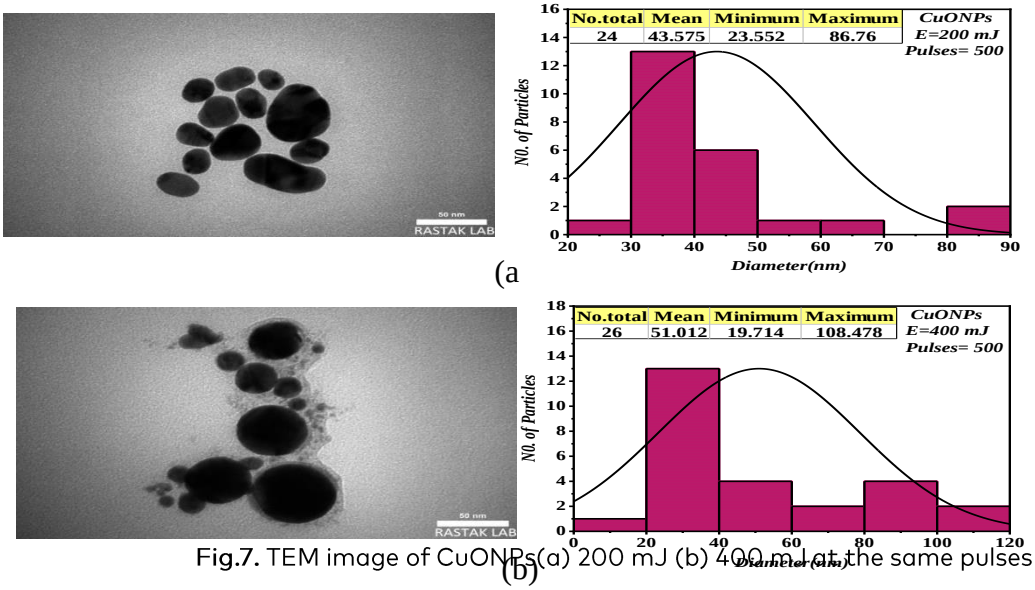

Fig.7. TEM image of CuONPs(a) 200 mJ (b) 400 mJ at the same pulses 500 (on the left side) and the particle size distribution (on the right side)

3.2.2.Atomic Force Microscopy (AFM)

The resulting map of surface topography by Atomic force microscopy technique has been done. AFM was used in a noncontact mode in an ambient environment to conduct studies on the properties of the nanosized structures of the deposited materials. In order to scan the thin film deposited on a p-type Si substrate at 100 ºC. The morphological properties study of sample gave a direct surface image of sample CuO prepared by PLAL method in three-dimensional at different laser energies with 500 pulses , and shows the statistical distribution of the particle size. The average grain size for CuNPs at 200 mJ is~48.27 nm while ~54.02 nm for 400 mJ with same number of pulses which is consistent with that obtained from TEM analysis

From Fig.8. depicts the particle size distributions and it is observed that the increased laser energy is accompanied by an increase in the size of nanoparticles. In addition, surface roughness increased as a function laser energies.

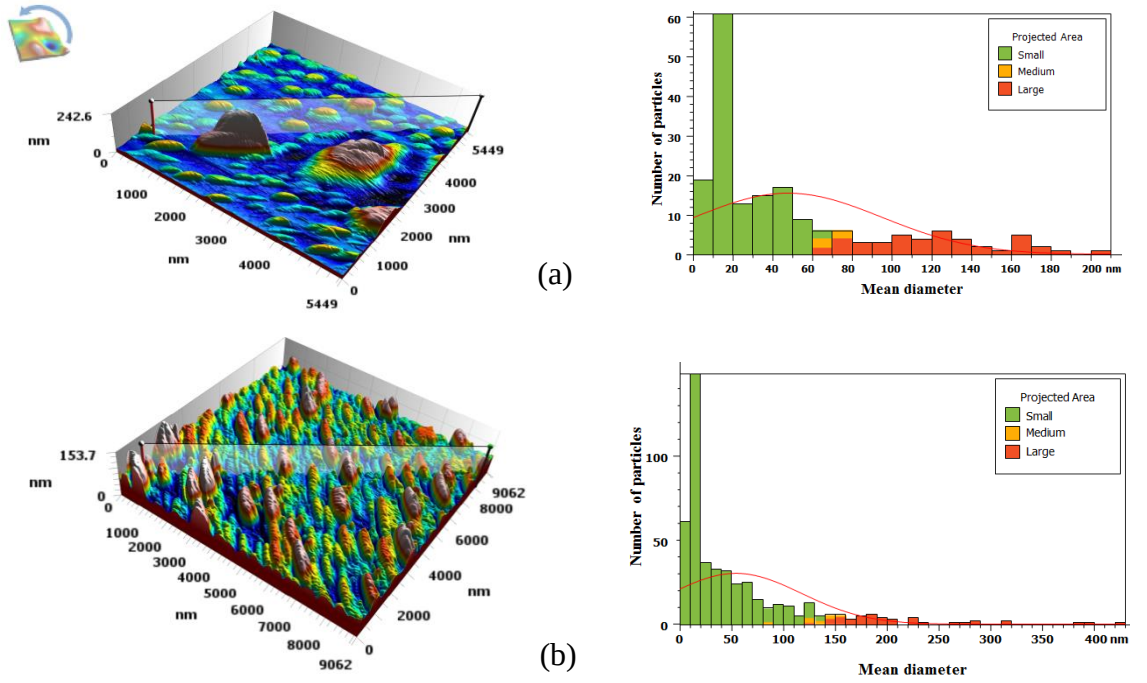

Fig.8. AFM analysis shows granularity cumulative distribution for CuONPs at ((a) 200 mJ and (b)400mJ) with 500 pulses.

4.Antibacterial activity of CuONPs

The present study investigates the antibacterial efficacy of CuONPs, synthesized via pulsed laser ablation in liquid (PLAL) at two different energy levels (200 and 400 mJ) with 500 pulses, against Bacillus cereus G(+ve) and Pseudomonas aeruginosa G(-ve) bacteria, utilizing the well diffusion method. The diameter of the inhibition zones for both bacterial strains was measured and recorded in millimeters, with the observed inhibition zones increasing with the concentration of CuONPs. The results of bacterial zones of inhibition, depicted in **Fig. 9**, indicate that the lower sensitivity of bacteria towards CuONPs is primarily attributed to the thickness of the peptidoglycan layer, which may hinder the penetration of nanoparticles through the bacterial cell wall (Ismail et al.,2018). Furthermore, the formation of nanoparticles through a PLAL technique that is minimal under realistic experimental conditions compared to other traditional techniques for synthesis nanoparticles (Yang,2012). Copper oxide nanoparticles come into contact with bacterial cells, they can penetrate the cell wall and disrupt the cell membrane, leading to the leakage of cellular contents and ultimately cell death. The phenomenon of electromagnetic attraction arises due to the interactions between the negative charges of microorganisms and the positive charges of nanoparticles. The interactions induce the oxidation of surface molecules present in microorganisms, ultimately leading to the death of bacteria (Shirsat et al., 2019).

Additionally, copper ions released from the copper oxide nanoparticles can also cause damage to bacterial DNA and interfere with cellular processes, further contributing to their antimicrobial activity. Our study reveals that CuONPs exhibit varying degrees of antibacterial activity, with the particles synthesized at 200 mJ being more effective against both bacterial strains, while the particles synthesized at 400 mJ with the same number of pulses exhibit few inhibition zones against P.aeruginosa as shown in **Table 1.** The observed variation in the resistance of B. cereus G(+ve) and P. aeruginosa G(-ve) bacterial cultures towards nanoparticles can be attributed to differences in their respective cell wall structures or degrees of contact with the size NPs.

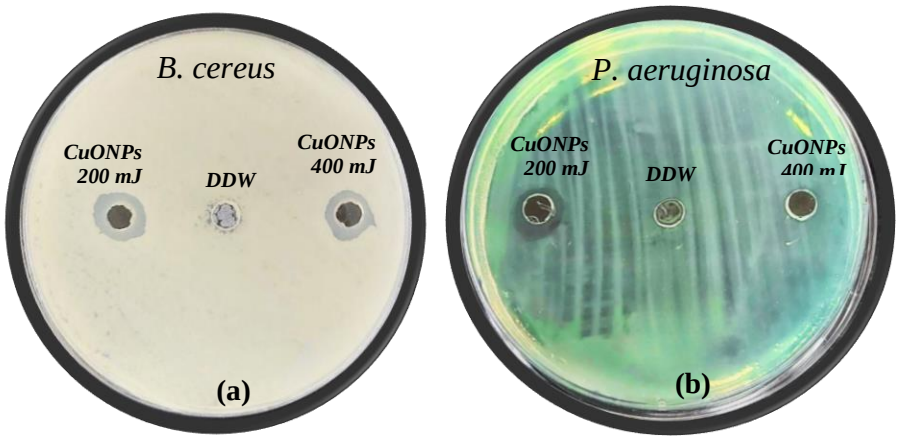

.

Fig.9 . The antibacterial activity test results for CuONPs prepared for 200 mJ and 400 mJ at a number of pulses as 500 (a) for Bacillus cereus G(+ve) (b) Pseudomonas aeruginosa G(-ve)

Table 1 Antibacterial activity of CuONPs against Bacillus cereus Pseudomonas aeruginosa respectively.

Bacterial strain	Sample with 500 pulses	Laser Energy (mJ)	zone inhibition (mm)
B. cereus	CuONPs	200	16
		400	14
P. aeruginosa	CuONPs	200	12
		400	7

5.Conclusions

By using the laser ablation technique on a copper target in double-distilled water, copper oxide nanoparticles can be easily produced. Several analyses were used to research and characterize the CuNPs. The absorbance increased with more pulses, according to UV-visible spectroscopy. The plasmon peak at 217 nm underwent a red shift as the number of laser pulses increased. The reaction of dissolved oxygen in water with the CuNPs produced the compounds associated with the oxidation of CuNPs into CuONPs. Copper oxide NPs papered at 400 mJ have a slightly higher absorbance intensity than samples papered at 200 mJ at the same number of pulses. CuNPs also have a sphecle-like morphology and diameters ranging from 46 to 52 nm for 200 mJ and 400 mJ, respectively. According to the findings of our study, copper oxide nanoparticles have a stronger antibacterial effect against both Bacillus cereus Pseudomonas aeruginosa respectively, when the laser energy is low and the same number of pulses. The findings suggest that CuONPs exhibit potential as a viable alternative for antibacterial agents and as a component in nanomedical applications.

Acknowledgements

The authors would like to express their warmest thanks to University of Mosul, College of Education for Pure Science, Department of Physics for supporting this work.

References

Al-Douri Y, Al-Samarai RA, Abdulateef SA, Odeh AA, Badi N, Voon CH. 2019. Nanosecond pulsed laser ablation to

synthesize GaO colloidal nanoparticles: optical and structural properties. Optik (Stuttg).;178:337–42.

Allaker, R.P., 2010. The use of nanoparticles to control oral biofilm formation. Journal of dental research, 89(11), pp.1175-1186.

Arakelyan, S. M., Veiko, V. P., Kutrovskaya, S. V., et al.,2016. Reliable and well-controlled synthesis of noble metal nanoparticles by continuous wave laser ablation in different liquids for deposition of thin films with variable optical properties . J Nanopart Res. 18, 155. https://doi.org/10.1007/s11051-016-3468-0

Azam, A., Ahmed, A.S., Oves, M., Khan, M.S. and Memic, A., 2012. Size-dependent antimicrobial properties of CuO nanoparticles against Gram-positive and-negative bacterial strains. International journal of nanomedicine, pp.3527-3535

Azadi, H., Aghdam, H.D., Malekfar, R. and Bellah, S.M., 2019. Effects of energy and hydrogen peroxide concentration on structural and optical properties of CuO nanosheets prepared by pulsed laser ablation. Results in Physics, 15, p.102610

Bhardwaj, A.K., Kumar, V., Pandey, V., Naraian, R. and Gopal, R., 2019. Bacterial killing efficacy of synthesized rod shaped cuprous oxide nanoparticles using laser ablation technique. SN Applied Sciences, 1, pp.1-8.

Carlin, F., M. Fricker, A. Pielaat, S. Heisterkamp, R. Shaheen, M. S. Salonen, B. Svensson, C. Nguyen-The, and M. EhlingSchulz. 2006. Emetic toxin-producing strains of Bacillus cereus show distinct characteristics within the Bacillus cereus group. Int. J. Food Microbiol. 109:132–138

Dufrenne, J., A. Tatini, and S. Notermans. 1994. Stability of spores of Bacillus cereus stored on silicagel. Int. J. Food Microbiol. 23:111–116.

El Zowalaty M.E, Al Thani A.A, Webster TJ, El Zowalaty A.E, Schweizer H.P, Nasrallah G.K, Marei H.E, Ashour H.M. . 2015. Pseudomonas aeruginosa: arsenal of resistance mechanisms, decades of changing resistance profiles, and future antimicrobial therapies. Future Microbiol.10(10):1683–706. http://dx.doi.org/10.2217/fmb.15.48

Ganeev RA, Baba M, Ryasnyansky AI, Suzuki M, Kuroda H. 2004. Characterization of optical and nonlinear optical properties of silver nanoparticles prepared by laser ablation in various liquids. Opt Commun;240(4–6):437–48.

Giorgetti E, Muniz Miranda M, Caporali S, Canton P, Marsili P, Vergari C, et al. 2015. TiO2 nanoparticles obtained by laser ablation in water: influence of pulse energy and duration on the crystalline phase. J Alloy Compd;643(S1):S75–9.

Gondal, M.A., Qahtan, T.F., Dastageer, M.A., Saleh, T.A., Maganda, Y.W. and Anjum, D.H., 2013. Effects of oxidizing medium on the composition, morphology and optical properties of copper oxide nanoparticles produced by pulsed laser ablation. Applied surface science, 286, pp.149-155.

Halbus, A.F., Horozov, T.S. and Paunov, V.N., 2019. Strongly enhanced antibacterial action of copper oxide nanoparticles with boronic acid surface functionality. ACS applied materials & interfaces, 11(13), pp.12232-12243.

Ismail, R.A., Sulaiman, G.M., Mohsin, M.H. and Saadoon, A.H., 2018. Preparation of silver iodide nanoparticles using laser ablation in liquid for antibacterial applications. IET nanobiotechnology, 12(6), pp.781-786.

Kareem, M.M., 2021. The Effect of Laser Shots on Morphological and Optical Properties of Copper Oxide NPs Prepared by Nd-Yag Laser of 1064 nm Wavelengths in Distilled Water. Passer Journal of Basic and Applied Sciences, 3(2), pp.200-206.

Mafuné, F., Kohno, J.Y., Takeda, Y., Kondow, T. and Sawabe, H., 2001. Formation of gold nanoparticles by laser ablation in aqueous solution of surfactant. The Journal of Physical Chemistry B, 105(22), pp.5114-5120.

Menazea, A. A., Elashmawi, I. S., El-kader, F. A., Hakeem, N. A., 2018. Nanosecond pulsed laser ablation in liquids as new route for preparing polyvinyl carbazole/silver nanoparticles composite: spectroscopic and thermal studies. J Inorg Organomet Polym . 28, 2564–2571. https://doi.org/10.1007/s10904-018-0890-z.

Monteiro, D.R., Gorup, L.F., Takamiya, A.S., Ruvollo-Filho, A.C., de Camargo, E.R. and Barbosa, D.B., 2009. The growing importance of materials that prevent microbial adhesion: antimicrobial effect of medical devices containing silver. International journal of antimicrobial agents, 34(2), pp.103-110.

Nie, S., Emory,S. R.,1997. Probing Single Molecules and Single Nanoparticles by Surface-Enhanced Raman Scattering .Science. 275, 1102-1106. DOI: 10.1126/science.275.5303.1102

Niu, K.Y., Yang, J., Kulinich, S.A., Sun, J., Li, H. and Du, X.W., 2010. Morphology control of nanostructures via surface reaction of metal nanodroplets. Journal of the American Chemical Society, 132(28), pp.9814-9819.

Pena C, Suarez C, Tubau F, Dominguez A, Sora M, Pujol M, Gudiol F, Ariza J. 2009. Carbapenem-resistant Pseudomonas aeruginosa: factors influencing multidrug-resistant acquisition in non-critically ill patients. Eur J Clin Microbiol Infect Dis.28(5):519–22. http://dx.doi.org/10.1007/s10096-008-0645-9

Patra N, Akash K, Shiva S, Gagrani R, Rao HSP, Anirudh VR, et al. 2016. Parametric investigations on the influence of nano-second Nd 3+ :YAG laser wavelength and fluence in synthesizing NiTi nano-particles using liquid assisted laser ablation technique. Appl Surf Sci;366:104–11.

Shirsat, S., Pawar, D.N., Jain, N., Pawar, J., Tale, V.S., & Henry, R.

2019. Synthesis of copper oxide nanoparticles by chemical precipitation method for the determination of antibacterial efficacy against Streptococcus sp. and Staphylococcus sp. Asian Journal of Pharmaceutical and Clinical Research, 135-138.

Tauc, J., Grigorvici , R., Vancu , A.,1966. Optical properties and Electronic structure of Amorphous Germanium . Phys. Status solid B ,15, 627-637. DOI: 10.1002/pssb.19660156224.

Triloki., Rai, R., Singh, B.K., 2013. Absorbance and Transmittance measurement of CsI thin films, Proceedings of the DAE Symp. on Nucl. Phys. 58, 838-839.

Yang .G. 2012.Laser ablation in liquids: principles and applications in the preparation of nanomaterials. CRC Press. p. 1192.

Zeng, H., Cai, W., Li, Y., Hu, J. and Liu, P., 2005. Composition/structural evolution and optical properties of ZnO/Zn nanoparticles by laser ablation in liquid media. The Journal of Physical Chemistry B, 109(39), pp.18260-18266.

Zeng, H., Xu, X., Bando, Y., Gautam, U.K., Zhai, T., Fang, X., Liu, B. and Golberg, D., 2009. Template Deformation-Tailored ZnO Nanorod/Nanowire Arrays: Full Growth

Control and Optimization of Field-Emission. Advanced Functional Materials, 19(19), pp.3165-3172.

Zhang, Q., Zhang, K., Xu, D., Yang, G., Huang, H., Nie, F., Liu, C. and Yang, S., 2014. CuO nanostructures: synthesis, characterization, growth mechanisms, fundamental properties, and applications. Progress in Materials Science, 60, pp.208-337.

Zoolfakar, A.S., Rani, R.A., Morfa, A.J., O'Mullane, A.P. and Kalantar-Zadeh, K., 2014. Nanostructured copper oxide semiconductors: a perspective on materials, synthesis methods and applications. journal of materials chemistry c, 2(27), pp.5247-5270.